Separation of Solutes from Aqueous Solutions by Contained Liquid Membranes

The hollow fiber contained liquid membrane (CLM) is a thin liquid film contained in the interstices of two sets of intermingled microporous hollow fine fibers. Organic CLM-s have been used here for the separation of solutes from an aqueous feed into an aqueous strip. Solutes studied are phenol and acetic acid. The separations are carried out in either hydrophilic or hydrophobic hollow fiber CLM permeator modules, using a variety of organic liquids (e.g., decanol, methyl isobutyl ketone, xylene) as membranes. First-order models have been developed to predict the overall solute transfer coefficients adequately. The transfer coefficient can be enhanced significantly when a chemical reaction is carried out on the strip side using NaOH. The advantages of the CLM structure include operational stability, independent control of membrane phase pressure, automatic replenishment of the lost membrane liquid, and absence of the need for preequilibration. These features are demonstrated here, even for systems with considerable aqueous-organic mutual solubilities.

A. Sengupta, R. Basu, K. K. Sirkar
Department of Chemistry
and Chemical Engineering
Center for Membranes
and Separation Technologies
Stevens Institute of Technology
Hoboken, NJ 07030

Introduction

Organic liquids immobilized in inert microporous supports can be used to transfer a solute between two aqueous solutions (Bloch, 1970). Such and other supported liquid membranes (SLM) have been studied for a number of years (Lonsdale, 1982) as selective separation barriers. Various applications of SLM-s for liquid separations have been investigated (Kuo and Gregor, 1983; Danesi, 1984–85; Nishiki and Bautista, 1985; Majumdar and Stroeve, 1986; Babcock et al., 1986). Extensive reviews are also available (Marr and Kopp, 1982; Way et al., 1982; Danesi et al., 1984–85).

The SLM-s have many inherent advantages. High stage separation factors can be achieved; the capital and operating costs, and energy requirements are low; fewer moving parts are used, resulting in less maintenance costs. Extractant loss due to poor coalescence, a major problem in conventional separation by solvent extraction, is totally eliminated. Compact and modular hollow fiber devices can be used with exceptionally high mass transfer area per unit equipment volume. Besides, the mass transfer rate can be enhanced using reversible and irreversible chemical reactions. Despite such obvious advantages, SLM-s have not been adopted for larger scale industrial processes, due primarily to the lack of their long term stability.

The probable causes of membrane instability are (Danesi, 1984–85; Danesi et al., 1987):

1) Loss of membrane by solubility in the mobile feed and strip phases.

2) Progressive wetting of the support pores by surface-active carrier molecules.

3) Pressure differential across the membrane.

4) Osmotic flow of large quantities of water across the membrane.

It is worthwhile to explore new liquid membrane structures that are stable and can retain the inherent SLM advantages.

Majumdar et al. (1988a) have recently proposed a new liquid membrane structure using hydrophobic microporous hollow fibers called Hollow Fiber Contained Liquid Membrane (HFCLM). This HFCLM appears to be able to overcome most of the shortcomings of aqueous SLM-s in gas separation. The present work explores the HFCLM separation for aqueous feed solutions and organic liquids membranes.

Aqueous liquid membranes that do not wet hydrophobic hollow fiber substrates can easily be contained in between the fibers for gas separations. Containing organic liquid membranes for aqueous solution separation is much more complicated since

Correspondence concerning this paper should be addressed to K. K. Sirkar.

organic liquids may wet both hydrophobic and hydrophilic substrates, either of which can be used. A number of competing configurations are thus realizable. Recent studies on interface immobilization in aqueous-organic systems for dispersion-free solvent extraction provide a systematic basis for developing such configurations (Kiani et al., 1984; Prasad and Sirkar, 1987a,b). Further, unlike in gas separation, the mass transfer resistances of the porous substrate and the fiber lumen boundary layers become important. Besides, chemical reactions can occur not only in liquid membrane but also in the feed or strip phases.

We first describe here the CLM configurations for microporous hollow fibers that can be either *hydrophilic* or *hydrophobic*. We then propose a first-order mass transfer model for solute transport without chemical reaction and identify the contributions of component resistances for a number of systems with a wide range of distribution coefficients. Experimental data on separation of phenol and acetic acid from aqueous solutions are reported next for organic membrane liquids, e.g., methyl isobutyl ketone (MIBK), decanol, and xylene. The variation of mass transfer coefficients with fiber lumen Reynolds numbers have been investigated. The stability and robust nature of the process is demonstrated with the MIBK-water system where there is considerable aqueous-organic mutual solubility.

CLM Configurations

Figure 1 shows schematically a cylindrical shell with a dense population of two sets of *hydrophilic* microporous fine hollow fibers separated at the ends. The microporous hollow fiber wall is called the substrate. The aqueous feed solution flows through the fibers marked 'F.' The aqueous strip solution flows through the fibers marked 'S.' The aqueous solutions will wet the hydrophilic fibers. The interstices of the fiber assembly in the permeator shell is filled with the organic membrane liquid (immiscible with the aqueous phases) at a pressure higher than the aqueous phase pressures. This is done by keeping the permeator shell connected to an outside membrane liquid reservoir under pressure, Figure 2.

Studies on nondispersive solvent extraction using microporous substrates (Kiani et al., 1984; Prasad and Sirkar, 1987a,b, 1988) indicate that a stable aqueous-organic interface is established if the pressure of the organic phase outside the pores is higher than that of the aqueous phase inside the pores, but lower than that required to displace the aqueous phase from the pores. Such conditions for aqueous-organic interface stabilization and

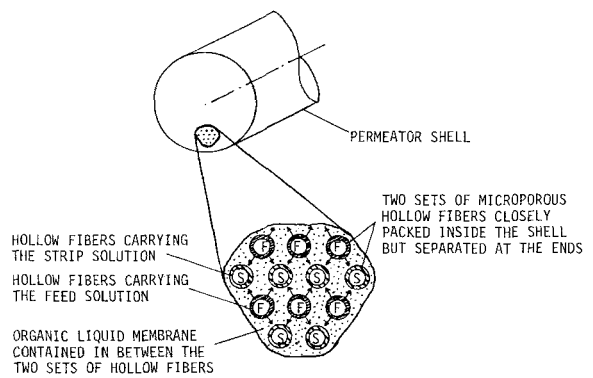

Figure 1. Structure of a contained liquid membrane (CLM).

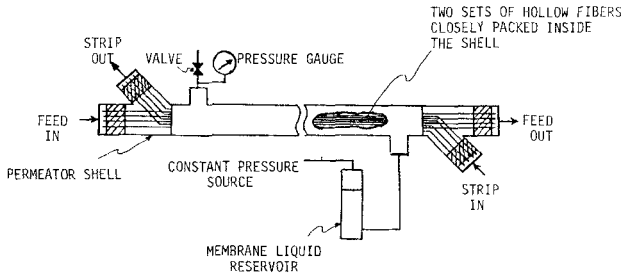

Figure 2. Flow schematic in a hollow fiber contained liquid membrane (HFCLM) permeator.

immiscible displacement in a porous media are independently available (Dullien, 1979). In the present case, two stable phase interfaces are created at the substrate pore mouths on the outside surface of the feed and the strip fibers, Figure 3. The liquid in the fiber interstices does not have any definite thickness; the mass transport path length from feed stream to strip stream is not unique, Figure 3. However, it functions exactly as a membrane contained between the feed and the strip, and hence the name CLM.

The solute is extracted from the feed into the liquid membrane at the feed-membrane interface and diffuses through the membrane to the nearest strip fiber(s). At the strip-membrane interface, the solute is back extracted into the strip phase. The solute diffusion through the two substrates is an integral part of the CLM mass transfer. Note that the actual membrane phase does not penetrate the hollow fiber wall, a condition totally different from the SLM configuration.

Since the shell is connected to a constant pressure source, any loss of membrane liquid is automatically replenished from the reservoir. If there are defects in the fibers, there may be leakage of membrane liquid into feed or strip phase, but separation remains basically unaffected since the membrane is not destroyed. The same is true if there is a surge in membrane liquid pressure. Leakage in the opposite direction is not possible since

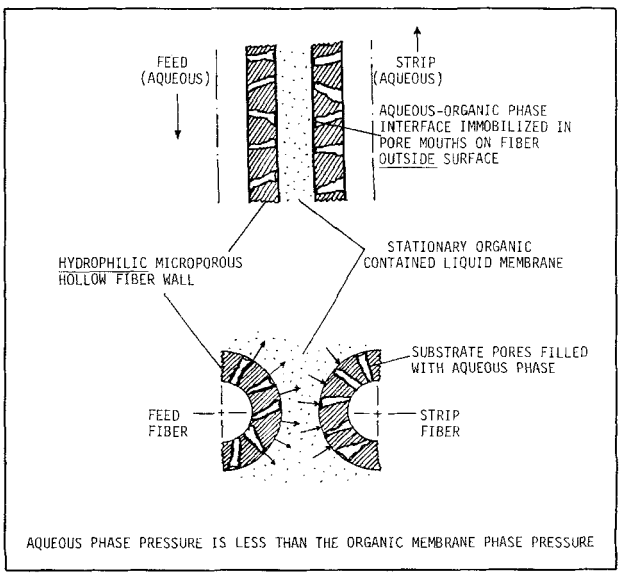

Figure 3. Phase interfaces in CLM for *hydrophilic* substrates.

the membrane is at a higher pressure. If there is a surge in feed (or strip) pressure, the feed or the strip may leak into membrane phase. However, the shell liquid can be removed from the other port on the shell side through a valve without interrupting the operation.

At any cross section inside the permeator, the relative positions between a feed fiber and the surrounding strip fibers (or vice versa) are not unique. A number of different configurations are probable. As a result, there is no well defined membrane thickness. The 'effective' membrane thickness in a given configuration can be estimated, however, based on the solution of two-dimensional diffusion equation in the liquid between the curved boundaries (Majumdar, 1986; Majumdar et al., 1988b). This effective membrane thickness depends mainly on: 1) the average center-to-center distance between any two adjacent fibers; and 2) the fiber outside diameter. The smaller the fiber outside diameter, smaller is the membrane thickness. An overall effective membrane thickness is estimated by averaging over different configurations. In a densely packed assembly of fine hollow fibers, it is possible to have a quite small effective membrane thickness.

Hydrophobic microporous hollow fibers can also be used to create a HFCLM. The substrate pores will then be filled with the organic membrane phase, instead of the aqueous phases, Figure 4. The feed and strip pressures will have to be higher than the membrane pressure to achieve stable phase interfaces on the *inner* surfaces of the hollow fibers. This again follows from earlier studies on nondispersive solvent extraction using microporous hydrophobic supports (Kiani et al., 1984; Frank and Sirkar, 1985; Prasad et al., 1986; Prasad and Sirkar, 1987a; Prasad and Sirkar, 1988). Since the membrane extends into the fiber walls, the effective membrane thickness will include the substrate thicknesses also.

Mass Transfer Coefficients

The solute concentrations in the feed, strip and membrane phases vary along the permeator length. Besides, the mass transfer patterns are uneven because of the curved fiber surfaces. Additionally, there are uncertainties regarding the effect of solute concentration on its distribution coefficient, the true diffusivities inside the tortuous substrate pores, and two-dimensional effects as the solute diffuses from the bulk into the pores, and vice versa. We believe that an exact mass transport analysis is not warranted at this initial stage of such a new technique. It is appropriate to use conventional mass transfer coefficients based on a "resistances-in-series" approach. The advantage is that it serves as a first-order means of rapid characterization of the separation process, and highlights the effects of some important parameters. Such an approach has yielded rich dividends in studies of nondispersive solvent extraction with an immobilized interface. Similar benefits are expected in the analysis of HFCLM structure involving two immobilized interfaces.

The overall mass transfer coefficient will be a function of five individual transfer coefficients (corresponding to two aqueous boundary layers, two porous substrates, and the CLM), the fiber dimensions, the distribution coefficients, etc. The assumptions here are:

1) Permeator-averaged transfer coefficients can be used.

2) There are no chemical reactions, and there is simple solute partitioning.

3) Substrate coefficients can be obtained from solute diffusivity, substrate porosity, tortuosity and thickness (Prasad and Sirkar, 1988).

4) A single effective membrane thickness is valid for the whole permeator.

5) No two-dimensional effects occur, as the solute diffuses from the continuous phases (feed, strip, or membrane) into the substrate pores, or vice versa (Keller and Stein, 1967).

6) The boundary layer coefficients can be obtained from general mass transfer analyses inside nonporous tubes.

Typical solute concentration profiles are shown in Figure 5. In a HFCLM permeator, the number and size of feed fibers

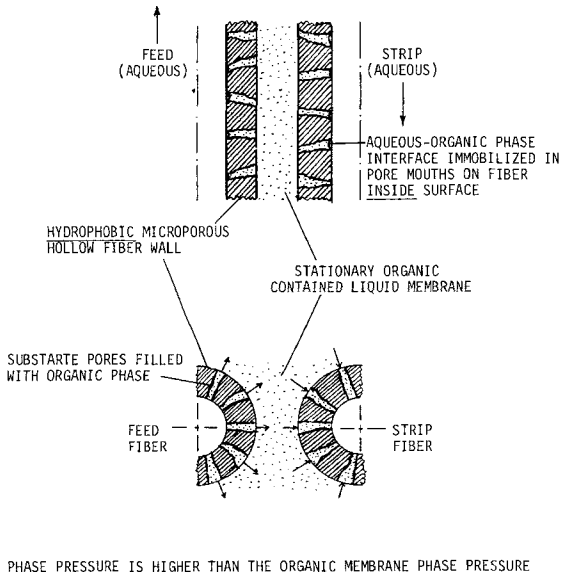

Figure 4. Phase interfaces in CLM for *hydrophobic* substrates.

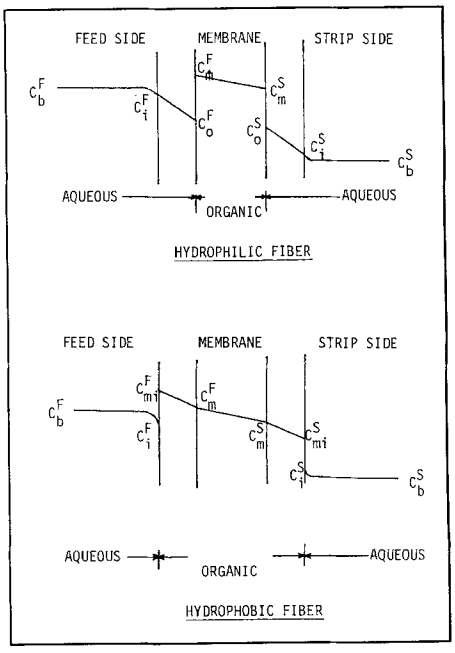

Figure 5. Typical solute concentration profiles for aqueous-organic-aqueous systems.

need not equal those for the strip fibers, and the feed-membrane and strip-membrane interfacial areas may be different (this actually is an advantage of CLM). A convenient way to define a simple and unique K_w, the aqueous phase based overall mass transfer coefficient, for hydrophilic substrate is as follows:

$$R_T = K_w(\pi d_o^F N_F C_b^F - \pi d_o^S N_S C_b^S) \tag{1}$$

where R_T is the solute transport rate per unit permeator length. It is related to the individual transfer coefficients as follows:

$$R_T = \pi d_i^F N_F k_w^F (C_b^F - C_i^F) \tag{2a}$$

$$= \pi d_{lm}^F N_F k_{sw}^F (C_i^F - C_o^F) \tag{2b}$$

$$= k_{mo}(\pi d_o^F N_F C_m^F - \pi d_o^S N_S C_m^S) \tag{2c}$$

$$= \pi d_{lm}^S N_S k_{sw}^S (C_o^S - C_i^S) \tag{2d}$$

$$= \pi d_i^S N_S k_w^S (C_i^S - C_b^S) \tag{2e}$$

Note that Eq. 2c is defined the same way as Eq. 1. Also,

$$C_m^F = m_D^F C_o^F; \quad C_m^S = m_D^S C_o^S \tag{3}$$

From the above equations, one can develop the following general expression for K_w for *hydrophilic* substrate:

$$\frac{1}{d_o^F K_w} + \frac{\pi}{R_T}\left(1 - \frac{d_o^S m_D^S}{d_o^F m_D^F}\right) N_S C_o^S - \left(1 - \frac{d_o^S}{d_o^F}\right) N_S C_b^S = \frac{1}{d_i^F k_w^F} + \frac{1}{d_{lm}^F k_{sw}^F} + \frac{1}{d_o^F m_D^F k_{mo}} + \frac{1}{d_{lm}^S k_{sw}^S} + \frac{1}{d_i^S k_w^S} \tag{4}$$

Equation 4 can be simplified for the following conditions

$$d_o^F = d_o^S (= d_o); \quad m_D^F = m_D^S (= m_D); \quad d_i^F = d_i^S (= d_i); \quad d_{lm}^F = d_{lm}^S (= d_{lm}) \tag{5}$$

to

$$\frac{1}{K_w} = \frac{d_o}{d_i}\left(\frac{1}{k_w^F} + \frac{1}{k_w^S}\right) + \frac{d_o}{d_{lm}}\left(\frac{1}{k_{sw}^F} + \frac{1}{k_{sw}^S}\right) + \frac{1}{m_d}\frac{1}{k_{mo}} \tag{6}$$

The quantity k_{mo} and the substrate transfer coefficients k_{sw}^F and k_{sw}^S are obtained as follows:

$$k_{mo} = D_o/\delta_M \tag{7}$$

$$k_{sw}^F = k_{sw}^S = D_w \epsilon_s / [\tau_s (d_o - d_i)/2] \tag{8}$$

The boundary layer coefficients are obtained using the following general expression (Skelland, 1974), where k is either k_w^F or k_w^S, and N_{Sh}, N_{Re} and N_{Sc} are the average values for either feed or strip:

$$N_{Sh} = (kd_i/D_w) = 0.5(d_i/L) N_{Re} N_{Sc} \theta \tag{9}$$

where

$$\theta = \frac{1 - \sum_{j=1}^{j=\infty} \frac{-4B_j}{\beta_j^2}\left(\frac{d\phi_j}{dr_+}\right)_{r_+=1} \exp\left(\frac{-\beta_j^2(2L/d_i)}{N_{Re}N_{Sc}}\right)}{1 + \sum_{j=1}^{j=\infty} \frac{-4B_j}{\beta_j^2}\left(\frac{d\phi_j}{dr_+}\right)_{r_+=1} \exp\left(\frac{-\beta_j^2(2L/d_i)}{N_{Re}N_{Sc}}\right)} \tag{10a}$$

with

$$\beta_j = 4(j-1) + 8/3 \tag{10b}$$

and

$$-B_j(d\phi_j/dr_+)/2 = 1.01276\beta_j^{-1/3}, j = 1, 2, 3 \ldots \tag{10c}$$

Equations 9 and 10a represent the theoretically obtained series solution of the Graetz problem with constant wall concentration, fully developed parabolic velocity profile, and developing concentration profile. In the present case, the fiber wall concentration does change along permeator length. However, the above equations have been found to predict the boundary layer coefficients well enough in solvent extraction studies using the same hollow fibers (Prasad and Sirkar, 1988), and thus are expected to provide good first order estimates here also.

For *hydrophobic* substrate, the following equation can be developed corresponding to Eq. 6:

$$\frac{1}{K_w} = \left(\frac{1}{k_w^F} + \frac{1}{k_w^S}\right) + \frac{d_i}{d_{lm}}\frac{1}{m_D}\left(\frac{1}{k_{so}^F} + \frac{1}{k_{so}^S}\right) + \frac{d_i}{d_o}\frac{1}{m_D}\frac{1}{k_{mo}} \tag{11}$$

The substrate coefficients are obtained as in Eq. 8, but D_w is replaced by D_o as the substrate is filled with organic.

An order-of-magnitude analysis of Eqs. 6 and 11 reveals some interesting features. For hydrophilic fiber permeators and a system with $m_D \gg 1$, Eq. 6 shows the CLM resistance to be negligible compared to the other four resistances. The overall transfer coefficient will vary with feed and strip flow rates (the substrate coefficients being invariant with flow rates). Conversely for $m_D \ll 1$ the CLM resistance may control.

For hydrophobic fiber permeators, on the other hand, in cases of $m_D \gg 1$ only the boundary layer resistances will be controlling. By increasing the flow rates sufficiently, it may be possible to have very high transfer rates. But for $m_D \ll 1$, the substrate and the membrane resistances will be very high. From a comparison it can also be said that for $m_D \gg 1$, the hydrophobic fiber permeator will be superior, whereas for $m_D \ll 1$, the hydrophilic fiber permeator will be superior, if all other conditions are identical.

Chemical reaction in strip solution

An irreversible chemical reaction in the strip solution can enhance the transfer rate significantly by increasing the concentration driving force. Examples are reaction of caustic with citric acid transported across SLM (Babcock et al., 1986), and reaction of caustic with phenol transported across emulsion liquid membranes (Cahn and Li, 1974). In a CLM configuration with a fast strip phase reaction, the strip side boundary layer resistance is also eliminated. For hydrophobic substrate and for $m_D \gg 1$, the only mass transport resistance will be the feed side boundary layer resistance.

Experimental

Hydrophilic regenerated cellulose (RC) hollow fibers (CasChem Inc., Bayonne, NJ, and CD Medical Inc., Miami Lakes, FL) and hydrophobic polypropylene (PP) Celgard X-10 hollow fibers (Questar, Charlotte, NC) were used in making permeator modules. To make the permeator, a fiber bunch was prepared first. Two sets of fibers of known number and length, were

placed on top of each other, and carefully rolled together in the middle, while keeping the ends separated on the two sides. The fiber bunch was then introduced to the permeator shell. The shell was a S.S. nipple, 10 cm long and of 1.27 cm inside diameter with a Teflon sleeve (1.03 cm outside diameter, 0.61 cm inside diameter, 10 cm length) epoxy-bonded at its inside surface. The sleeve was used to prevent damage to the fibers by direct friction against the rough metal surface. The ends of the two sets of fibers were taken out separately on each side through the two arms of a Y-fitting, and potted with epoxy. There were separate openings on the shell for introduction and withdrawal of membrane liquid, as shown in Figure 2.

The geometric characteristics of the fibers and the permeators are shown in Table 1. Very high values of the surface area per unit volume (the so-called a values) can be obtained in these permeators. Note that in this case we used only half the total number of fibers in calculating a as there are two sets of fibers. The dimensions of the hydrophilic fibers are in unpressurized condition. It is likely that there were deformation of these fibers during experiments, as they are not mechanically very strong. The packing density value of 78% in one of the permeators was calculated from the wetted fiber dimensions in unpressurized condition (and so may not be correct), with a correspondingly low value of effective membrane thickness (Majumdar et al., 1988b).

The experimental setup is shown schematically in Figure 2. The different solute-membrane combinations used provide a wide range of m_D values, Table 2. Note that MIBK and water have considerable mutual solubilities (Won and Prausnitz, 1975). The experiments were carried out for hydrophilic as well as hydrophobic fiber permeators. Both cocurrent and countercurrent feed-strip flow patterns were employed.

The membrane phase pressure (shell pressure), and the inlet and outlet pressures of the feed and strip phases were monitored using dial gauges. The flow rates were controlled using regulating valves. At the beginning of each experiment, the flow rates and the phase pressures were established as quickly as possible,

Table 1. Geometric Characteristics of the Permeators

	Hydrophilic Batch 1	Hydrophilic Batch 2	Hydrophobic
Fibers	Regenerated cellulose	Regenerated cellulose	Polypropylene
Fiber Dimensions,* μm			
Outside diameter, d_o	200†	270†	150‡
Inside diameter, d_i	150	220	100
No. of fibers, N_F, N_S	200 Feed 200 Strip	200 Feed 200 Strip	300 Feed 300 Strip
Est. eff. CLM thickness, δ_M, μm**	120	40	110
Eff. permeator length, cm	10	10	10
Mass transfer area per unit volume (a), cm^{-1}	43.0	58.0	32.2
Fraction of shell cross-sectional area occupied by the two fibers sets***	0.43	0.78	0.36

*In wet condition, from manufacturer's data.
**From (Majumdar et al., 1988b).
***Calculated based on wet dimensions from manufacturer's data.
†Measured under optical microscope.
‡From manufacturer's data.

Table 2. Systems Studied

Liquid Membrane	Solute	Approx. Solute Conc. in Feed	Strip Solution	Distr. Coeff. (m_D) at Feed Conc.*
MIBK	Phenol	1% w/v	Water	35**
MIBK	Phenol	1% w/v	2% NaOH	35
Decanol	Phenol	1% w/v	Water	25†
MIBK	Acetic acid	3% w/v	Water	0.5‡
Xylene	Acetic acid	3% w/v	Water	0.012‡

*m_D values may vary considerably with solute concentration.
**Estimated from Won and Prausnitz (1975).
†Estimated from Kiezyk and Mackay (1973).
‡From Prasad et al. (1986).

and the system allowed to reach a steady state. On an average, 6 to 10 hours elapsed before taking the samples and measuring the flow rates for each data point.

The experimental ranges of flow rates, Reynolds Numbers, and pressures are listed in Table 3. Flow rates were mostly low, determined with measuring cylinders and timers. Acetic acid concentrations were measured by NaOH-titrations (Kiani et al., 1984). Phenol concentrations were determined using a Hewlett-Packard HPLC (model 1090), a reverse phase C-18 column with 35% acetonitrile – 65% water carrier and a UV detector at 280 nm wavelength. For caustic strip runs, the strip solution was 2% wt./vol. NaOH in water.

The experimental K_w values are calculated from transfer rates based on the steady state bulk removal of the solute from the feed:

Hydrophilic:

$$K_w \pi d_o L N_F \Delta C_{LM} = Q_F (C^F_{in} - C^F_{out}) \tag{12a}$$

Hydrophobic:

$$K_w \pi d_i L N_F \Delta C_{LM} = Q_F (C^F_{in} - C^F_{out}) \tag{12b}$$

where

$$\Delta C_{LM} = \frac{(C^F_{in} - C^S_{out}) - (C^F_{out} - C^S_{in})}{\ln [(C^F_{in} - C^S_{out})/(C^F_{out} - C^S_{in})]} \tag{12c}$$

for countercurrent feed/strip operation. For cocurrent operation, C^S_{out} should be replaced by C^S_{in} in Eq. 12c, and vice versa. Note that Eq. 12a uses d_o and Eq. 12b uses d_i.

Results and Discussion

First we indicate the diffusivities and distribution coefficients for each system studied, and estimate the individual mass transfer coefficients needed to predict K_w theoretically. We also identify the controlling resistances for mass transfer. We present next the experimental K_w values, and compare them with the theoretical predictions. Finally we discuss various other aspects of the CLM technique.

Table 4 lists the diffusivities (from Wilke-Chang correlation, Reid et al., 1977) and the distribution coefficients (m_D). The quantity m_D depends strongly on solute concentration for phenol-MIBK system (Won and Prausnitz, 1975). However, calcu-

Table 3. Flow Conditions of the Study

System Solute-Membrane	Feed Side Flow Rate Range mL/min	Feed Side N_{Re} Range	Strip Side Flow Rate Range mL/min	Strip Side N_{Re} Range
Hydrophilic				
Phenol-Decanol	0.22–8.0	0.11–3.86	1.4–8.4	0.7–4.05
Phenol-MIBK	0.23–9.4	0.11–4.53	1.8–8.5	0.87–4.10
Acetic Acid-Xylene	0.7–8.15	0.34–3.93	2.7–16.0	1.3–7.72
Acetic Acid-MIBK	0.05–0.09	0.03–0.04	0.06–0.14	0.03–0.07
Hydrophobic				
Phenol-Decanol	0.8–1.06	0.63–0.75	0.8–3.1	0.58–2.19
Phenol-MIBK	0.4–1.5	0.30–1.10	0.9–1.18	0.64–0.84
Acetic Acid-Xylene	0.03–0.78	0.02–0.55	0.37–0.71	0.26–0.51
Acetic Acid-MIBK	0.29–2.04	0.21–1.45	0.39–1.94	0.28–1.37

System Solute-Membrane	Pressure, kPa Feed Inlet	Feed Outlet	Membrane Phase	Strip Inlet	Strip Outlet
Hydrophilic					
Phenol-MIBK	31–41	8–39	46–50	9–28	0–24
Phenol-Decanol	21–48	0–45	41–65	28–41	0–21
Acetic Acid-MIBK	41–97	0–7	50–100	28–54	0
Acetic Acid-Xylene	33–43	7–32	55	26–46	0
Hydrophobic					
Phenol-MIBK	28–52	10–14	10	28–31	14–21
Phenol-Decanol	34–55	14–21	12–14	28–48	14–28
Acetic Acid-MIBK	28–48	14–28	3–10	24–28	17–28
Acetic Acid-Xylene	34–41	16–29	12	47–48	20–24

lations indicated that an average m_D value could be used in this case without any appreciable error in the results, as the contributions of the terms containing m_D were very minor. For other systems, the variation of m_D with concentration was not significant in our operating ranges.

Table 4 also shows the properties for the hydrophilic and the hydrophobic substrates. The ϵ_s value for hydrophilic substrate used in this study was arrived at by actual experimental measurement of the weight difference between the dry and the wet fibers (Prasad and Sirkar, 1988). The values of t_s for RC fibers, and ϵ_s and t_s for X-10 fibers are taken from the respective manufacturer's data. The tortuosity factors τ_s for RC and PP fibers are average estimates from previous solvent extraction (Prasad and Sirkar, 1988) and gas permeation (Bhave and Sirkar, 1986, 1987) studies, respectively.

Table 4. System Transfer Properties and Substrate Properties at 25°C

Diffusivities and Distribution Coefficients

Solute-Membrane	Est. Avg. Dist. Coeff. (m_D) mg/L/mg/L	Est. Solute Diffusivity in Water (D_w), cm²/s	Est. Solute Diff. in Organic (D_o), cm²/s
Phenol-MIBK	55	1.05×10^{-5}	2.65×10^{-5}
Phenol-Decanol	25	1.05×10^{-5}	1.63×10^{-6}
Acetic Acid-MIBK	0.5	1.24×10^{-5}	3.14×10^{-5}
Acetic Acid-Xylene	0.012	1.24×10^{-5}	2.50×10^{-5}

Substrate Properties

Substrate	Thickness $(t_s) = (d_o - d_i)/2$ μm	Porosity (ϵ_s)	Tortuosity Factor (τ_s)
Hydrophilic	25	0.5	5
Hydrophobic	25	0.2	3.5

The calculated mass transfer coefficients for the membrane and the two substrates are listed in Table 5. Each CLM coefficient reported is the product of m_D and the permeability k_{mo} (defined in Eq. 7). The substrates transfer coefficients are calculated using Eq. 8, with D_w replaced by D_o for hydrophobic fibers.

Table 5 indicates a wide variation in the values of transfer coefficients. The CLM transfer coefficients for the phenol-MIBK system (highest m_D value) and for the acetic acid-xylene system (lowest m_D value) are about four orders of magnitude different. As the effective membrane thickness decreases (from batch 1 to batch 2, hydrophilic fibers), the CLM coefficient naturally increases. However, as we will see shortly from Table 6, this increase is likely to affect the overall transfer coefficient only for $m_D \ll 1$, where the CLM resistance controls. For $m_D \gg 1$, the increase is practically of no consequence, indicating that the minimization of membrane thickness is of very little importance in these cases.

The substrate and CLM transfer coefficients are constant for each system, but the boundary layer coefficients k_w^F and k_w^S will vary with flow rates. To assess the importance of the boundary layer resistances, the contributions of different mass transfer resistances for each system are compared in Table 6 for two different flow rates. The values reported are percent of total resistance offered by each of the following three: 1) the two boundary layers; 2) the two substrates; and 3) the CLM. They are obtained by calculating the magnitudes of the corresponding terms on the right sides of Eqs. 6 and 11. The feed and strip flow rates (the total flow rates) are assumed to be equal in each calculation since the number and size of feed and strip fibers are identical.

Table 6 suggests that the percent resistance values may vary dramatically depending on the system and the substrate. For example, with the *hydrophilic* substrate, for acetic acid-xylene system the CLM resistance becomes most important at high flow rates. At the other extreme, for phenol-MIBK system the CLM resistance is all but negligible, and thus the aqueous substrate and boundary layer resistances become important. For *hydrophobic* substrate and phenol-MIBK system, the boundary

Table 5. CLM and Substrate Transfer Coefficients

System	CLM Transfer Coefficients ($m_D k_{mo}$), cm/s Hydrophilic Batch 1 $\delta_M = 120\ \mu m$	Hydrophilic Batch 2 $\delta_M = 40\ \mu m$	Hydrophobic $\delta_M = 110\ \mu m$
Phenol-MIBK	1.21×10^{-1}	3.64×10^{-1}	1.33×10^{-1}
Phenol-Decanol	3.39×10^{-3}	1.02×10^{-2}	3.70×10^{-3}
Acetic Acid-MIBK	1.31×10^{-3}	3.93×10^{-3}	1.43×10^{-3}
Acetic Acid-Xylene	2.50×10^{-5}	7.50×10^{-5}	2.73×10^{-5}

System	Substrate Transfer Coef. (k_s), cm/s Hydrophilic*	Hydrophobic**
Phenol-MIBK	4.20×10^{-4}	6.06×10^{-4}
Phenol-Decanol	4.20×10^{-4}	3.73×10^{-5}
Acetic Acid-MIBK	4.95×10^{-4}	7.18×10^{-4}
Acetic Acid-Xylene	4.95×10^{-4}	5.71×10^{-4}

*$k_s = (D_w \epsilon_s)/(t_s \tau_s)$.
**$k_s = (D_o \epsilon_s)/(t_s \tau_s)$ where $t_s = (d_o - d_i)/2$

Table 6. Relative Contributions of Different Mass Transfer Resistances

System Solute-Membrane	Flow Rate mL/min	% of Total Mass Transfer Resistance Offered by: Feed + Strip Boundary Layers	Two Substrates	CLM
Hydrophilic				
Phenol-MIBK	1	35.5%	64.5%	<0.04%
	10	6.9%	93.1%	~0.05%
Phenol-Decanol	1	35.0%	63.6%	1.4%
	10	6.7%	91.3%	2.0%
Acetic Acid-MIBK	1	37.8%	58.3%	3.8%
	10	7.1%	87.2%	5.7%
Acetic Acid-Xylene	1	12.7%	19.6%	67.6%
	10	1.8%	22.1%	76.1%
Hydrophobic				
Phenol-MIBK	1	99.0%	0.85%	0.09%
	10	92.4%	6.9%	0.7%
Phenol-Decanol	1	74.6%	23.0%	2.4%
	10	25.4%	67.6%	7.0%
Acetic Acid-MIBK	1	36.4%	57.7%	5.9%
	10	5.9%	85.3%	8.8%
Acetic Acid-Xylene	1	1.1%	89.7%	9.2%
	10	0.1%	90.6%	9.3%

layer resistances are crucial, whereas for acetic acid-xylene system with the same substrate, boundary layer resistances do not affect the overall mass transfer in any way.

Table 6 also indicates that the substrate resistances play major roles in many situations. In particular, for high m_D system with hydrophilic fibers, and for low m_D system with hydrophobic fibers, the substrates offer most of the mass transfer resistances. Substrate properties like t_s (fiber wall thickness), τ_s and ϵ_s determine the magnitude of the substrate resistance. Therefore, in substrate-controlled transport, substrates with more favorable values of t_s, τ_s and ϵ_s would enhance the separation.

Figure 6 plots the experimental and the predicted K_w values

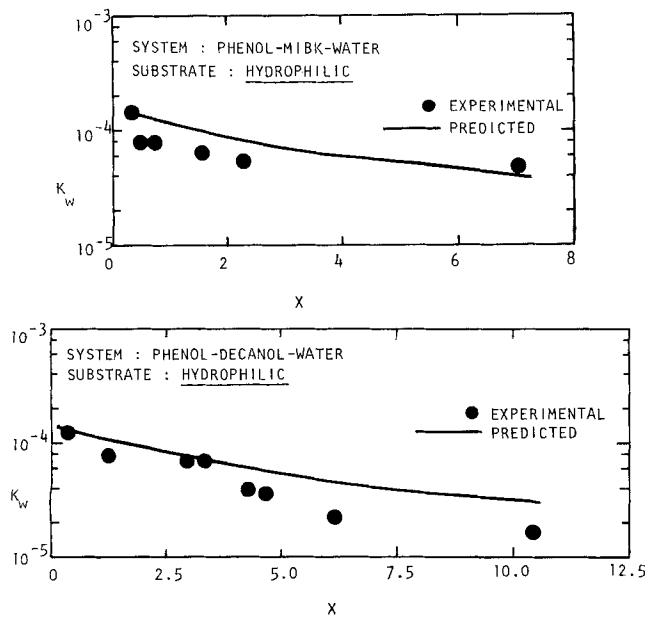

Figure 6. Experimental and predicted values of overall mass transfer coefficients for *hydrophilic* substrate: effect of flow variable *X*.

against the flow variable X defined as

$$X = (1/N_{Re}^{F}) + (1/N_{Re}^{S}) \tag{13}$$

The rationale for choosing a flow variable such as X instead of flow rates is that both the feed and the strip flow rates change from one data point to another, and the quantity X can effectively accomodate these simultaneous flow rate changes. The term K_w is plotted in Figure 6 instead of $1/K_w$ since the former is a more familiar quantity.

Figure 6 gives the results for phenol-MIBK and phenol-decanol systems with hydrophilic substrate. Results for both batch 1 and batch 2 hollow fibers have been plotted here. Note that these two permeators have different fiber diameters, and different effective CLM thickness, but have the same values of ϵ_s, t_s and τ_s (the substrate coefficients therefore remain the same). The results show that K_w values are not sensitive to the fiber dimensions, or packing density, indicating that the CLM thickness has little effect on the transfer rate in this situation, as predicted by the model. They show that as long as the substrate thickness remains the same, the fiber diameter has only a limited effect on K_w, which is also predicted by the model. It is also encouraging to find that the predicted and experimental K_w values are reasonably close. Also, a higher value of X means lower Reynolds numbers and lower flow rates, and as expected, K_w decreases at higher X. Note that by definition, two different sets of feed/strip flow rates can mean the same X value. Some data points in the figure therefore appear very close even though the flow conditions are actually very different.

Figure 7 plots K_w against X for the hydrophobic substrate. For phenol-MIBK, the predicted values match the data well, but for phenol-decanol system the discrepancies are higher for reasons unknown at this time. They probably point towards the inadequacies of the model, including the method of calculating the boundary layer coefficients. Besides, there are possible two-dimensional mass transfer effects in this case, since, unlike the other membranes studied here, decanol has a very high viscosity, and consequently the solute diffusivities in the membrane are

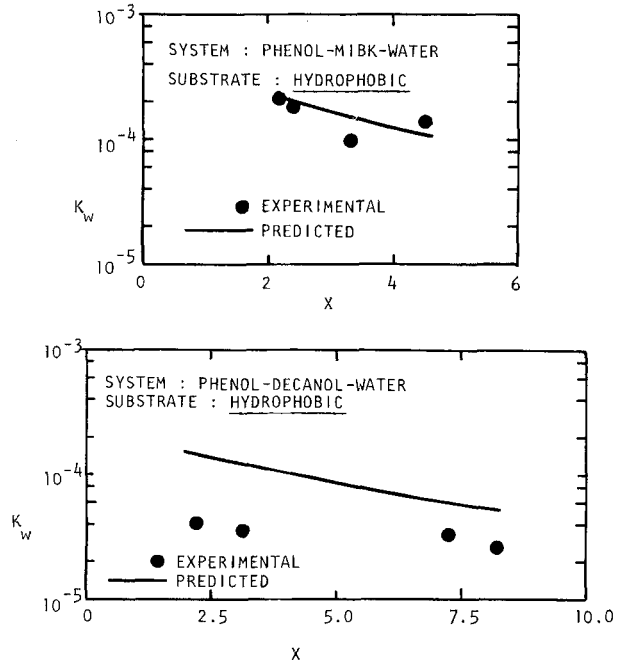

Figure 7. Experimental and predicted values of overall mass transfer coefficients for *hydrophobic* substrate: effect of flow variable *X*.

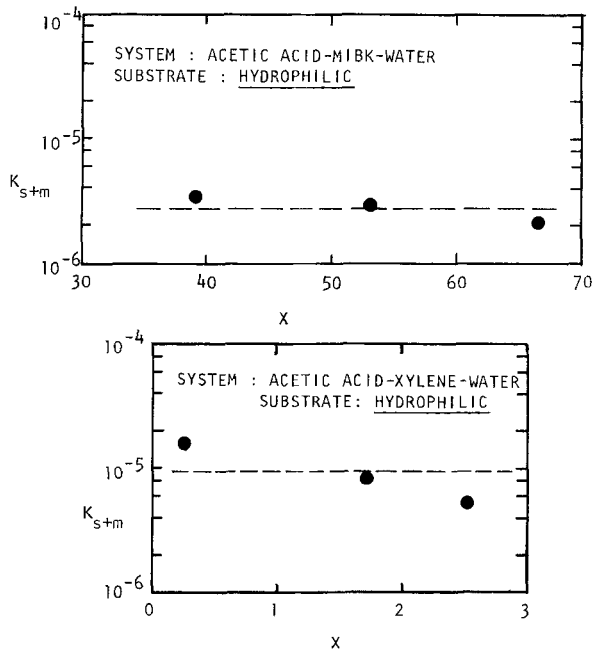

Figure 8. Combined substrate and membrane transfer coefficients for *hydrophilic* substrate: effect of flow variable *X*.

very low, and at the same time Celgard X-10 fibers have much lower porosity ($\epsilon_s = 0.20$) compared to the RC fibers (Keller and Stein, 1967).

For acetic acid systems also, the deviations between experimental and predicted K_w values are considerable. Note that for phenol systems ($m_D \gg 1$), errors in calculating the boundary layer coefficients are likely to affect the result much more than errors in selecting the value of say m_D. For acetic acid systems, the situation is somewhat opposite. Additionally, because of acetic acid ionization in the aqueous phases (particularly in the strip where the concentration is very low), the chosen m_D value may be inaccurate. Also, the measurement of very low acetic acid concentration in the strip solution may contribute to experimental inaccuracies.

For acetic acid system, one can test the model by defining a combined CLM-substrate coefficient K_{s+m} as follows,

Hydrophilic:

$$\frac{1}{K_{s+m}} = \frac{1}{(K_w)_{\text{expt}}} - \frac{d_o}{d_i}\left[\frac{1}{k_w^F} + \frac{1}{k_w^S}\right] \tag{14a}$$

Hydrophobic:

$$\frac{1}{K_{s+m}} = \frac{1}{(K_w)_{\text{expt}}} - \left[\frac{1}{k_w^F} + \frac{1}{k_w^S}\right] \tag{14b}$$

and plotting it against the flow parameter X. Ideally K_{s+m} should be a constant with X, since the flow-dependent terms are removed from K_w. Figures 8 and 9 confirm this well enough (except for xylene-HAc system) indicating that this aspect of the model is acceptable.

Consider now the magnitude of the mass transfer rates. Of all the four systems studied with water strip, phenol-MIBK with hydrophobic substrate gives the highest transfer coefficients, directly from the model, since it is a high m_D system, and the substrate and CLM resistances are practically negligible, Table 6. The K_w values are the lowest for the xylene-HAc system and hydrophobic substrate, as expected.

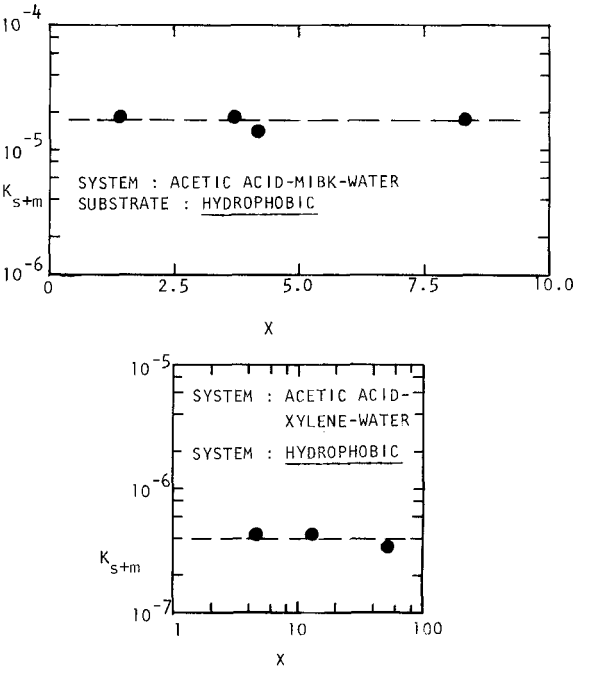

Figure 9. Combined substrate and membrane transfer coefficients for *hydrophobic* substrate: effect of flow variable *X*.

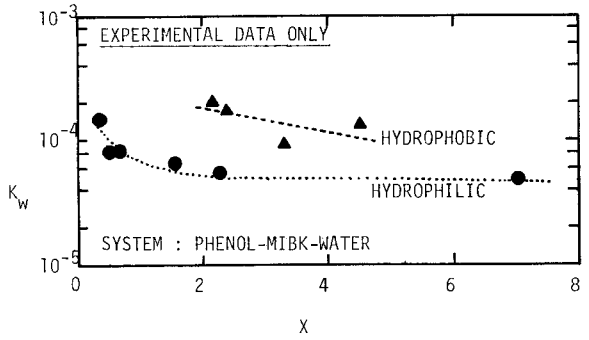

Figure 10. Effect of substrate types on experimental separation.

It is interesting that the CLM thickness becomes practically inconsequential for high m_D systems. For hydrophobic PP substrate the membrane penetrates the substrate, and the actual membrane thickness is the effective CLM thickness plus the thicknesses of the two substrates. However, contrary to expectations, this actually improves the K_w value compared to the RC fibers as indicated in Figure 10 which compares the K_w for the two substrates for similar conditions. This follows directly from the model, since when the substrates are filled with the membrane for high m_D system, their mass transfer resistances actually decrease. Additionally, for high m_D hydrophobic system, the separation becomes boundary layer controlled and in order to improve the stage separation factor, one needs to decrease the hydrodynamic mass transfer resistance rather than the membrane or substrate resistances.

Figure 11 and Table 7 explore the extent to which a caustic strip can improve the separation. Only experimental data are presented. Figure 11 compares K_w values with or without caustic strip for phenol-MIBK system, and indicates the beneficial effect of a downstream irreversible reaction on overall separation. The latter is also illustrated in Table 7 which lists the experimental Reynolds numbers and the corresponding K_w values.

For caustic strip, one should consider the reaction enhancement of mass transfer coefficient, instead of using a simple boundary layer coefficient. The flow parameter X is still used in Figure 11, however, for the sake of comparison. Actually, a concentrated caustic strip would eliminate the strip boundary layer resistance, and the contribution of the strip term in X would be negligible. Therefore, the curve for caustic strip will effectively shift to the left, and will actually highlight the fact that caustic

Table 7. Results for Water Strip vs. 2% NaOH Strip

Water strip			2% NaOH strip		
N_{Re}^F	N_{Re}^S	K_w, cm/s (Experimental)	N_{Re}^F	N_{Re}^S	K_w, cm/s (Experimental)
0.57	0.64	9.50×10^{-5}	0.39	0.11	2.37×10^{-4}
0.95	0.74	1.77×10^{-4}	0.41	0.12	2.86×10^{-4}
1.07	0.80	2.06×10^{-4}	0.83	0.20	3.33×10^{-4}
0.30	0.84	1.36×10^{-4}	0.33	0.12	2.12×10^{-4}

improves separation more than what is apparent in the figure. The numbers in Table 7 point out more directly that even for much lower feed Reynolds number values, the caustic strip yields much higher overall transfer coefficients. Under identical flow conditions, caustic strip may give K_w values which are 3–5 times as much as those for water strip.

In absolute magnitudes, the transfer coefficients K_w-s obtained in HFCLM permeators are usually lower compared to those in some traditional separation processes and devices. However, the overall separation efficiency is determined by the magnitude of the product $K_w a$. The greatest advantage of hollow-fiber-based devices in general is that exceptionally high value of a may be achievable, which in most cases can more than compensate for the low K_w values (Matson et al., 1983; Kiani et al., 1984; Prasad and Sirkar, 1988; Dahuron and Cussler, 1988).

A relative evaluation of the mass transfer rates in HFCLM permeators with those in other types of membrane processes will be useful. For comparison we may choose the liquid emulsion membrane (LEM) process, described in Cahn and Li (1974), for phenol separation with a caustic receiving phase. They have used the quantity $D'(V_E/V_W)$ where D' is the effective permeation rate constant, and V_E/V_W is the treat ratio. Based on their definition, this quantity is equivalent to $K_w a$ in the present case. For a receiving phase of 10% caustic, a typical experimental D' value was 1.7 min^{-1} with $V_E/V_W = 0.532$, yielding $D'(V_E/V_W)$ equal to $\simeq 0.90$ min^{-1}. In our study a typical experimental K_w value for 2% caustic strip solution, Table 7, is 3×10^{-4} cm/s. Assuming $a = 32$ cm^{-1}, Table 1, we find $K_w a \simeq 3 \times 10^{-4} \times 32 \times (60 \text{ s/min}) = 0.58$ min^{-1}. Since significantly higher a values are achievable in hollow-fiber-based devices (Matson et al., 1983), it is obvious that the mass transfer rates in CLM permeators can become truly comparable with those in the LEM separator.

Two more points should be considered. Firstly, for the high m_D system in particular, the actual CLM mass transfer resistance is negligible and the overall transfer coefficient is dependent only on the mobile phase hydrodynamics. If one can mini-

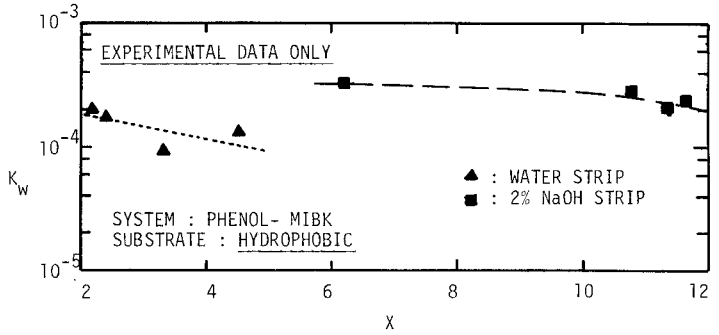

Figure 11. Effect of caustic strip on experimental separation.

mize the boundary layer resistances, much higher K_w values can be achieved. Secondly, since K_w does not depend on CLM thickness or the fiber packing density, increasing the capacity does not decrease the separation efficiency. Scale-up should therefore be much easier. These factors, combined with some of the other advantages of the CLM structure described earlier, make it worthwhile to explore the CLM liquid separation processes further.

Finally, a few words about the stability of the CLM process need to be mentioned. It is especially significant to note that there were very few problems in the long-time operation with the MIBK membrane, although there is a substantial solubility of the membrane liquid MIBK in the mobile water phases (in fact without MIBK addition from the membrane liquid reservoir, the liquid membrane would disappear in a few hours). We carried out a 44-hour continuous run with acetic acid-MIBK system without any problem. For the decanol system, we deliberately ran a RC fiber permeator with some defective strip fibers continuously for 42 hours without a decrease in separation. We also ran a PP fiber permeator continuously for 72 hours with decanol membrane. Such a robust structure is the essential requirement for larger-scale adoption of liquid membranes in process industries.

Conclusions

Solutes can be separated from aqueous feed to aqueous strip solutions conveniently using organic contained liquid membranes (CLM). These are thin organic films contained in the interstices of two sets of microporous hollow fine fibers. The robust and stable nature of these CLM membranes have been experimentally demonstrated for solutes phenol and acetic acid in various systems, including one with high mutual aqueous-organic solubilities. The CLM permeators can be constructed using either hydrophilic or hydrophobic hollow fibers. High membrane surface area per unit volume is achieved easily in these modules. The use of a strip solution containing 2% NaOH showed significant enhancement of mass transfer coefficient for phenol separation.

The CLM structure allows independent control of pressure in each phase (aqueous or organic). Maintaining the proper phase pressures is the chief requirement for successful operation. For hydrophilic fiber permeators with aqueous phase in the fiber wall pores, the pressure of the organic liquid membrane must be higher than that of the aqueous phases. For hydrophobic fiber permeators with the organic liquid membrane in the pores, the reverse is true. In both the cases, the pressure differential between the phases must be less than the breakthrough pressure.

First-order models have been developed for solute transport in CLM permeators. The mass transfer resistances of the contained liquid membrane, the microporous hollow fiber substrates, and the fiber lumen boundary layers have been incorporated. The model predictions generally agree well with the experimental mass transfer coefficients. For systems with low solute distribution coefficients ($m_D \ll 1$) and for hydrophilic hollow fiber permeators, the mass transfer resistance of the CLM controls. On the other hand, for systems with high solute distribution coefficients ($m_D \gg 1$) and for hydrophobic fiber permeators, the fiber lumen boundary layer resistances are likely to control.

Acknowledgment

We are grateful to Robert W. Callahan of Questar Inc., Charlotte, NC, and Ellen Craven of CD Medical Inc., Miami Lakes, FL, for supplying us with Celgard X-10 hollow fibers, and SCE-Cellulose hollow fibers, respectively.

Notation

a = mass transfer area per unit permeator volume, cm^{-1}
b_j, B_j ($d\phi_j/dr_+$) = constants, Eqs. 10b and 10c
C^F_{in}, C^F_{out} = solute concentration in the feed inlet and feed outlet, respectively, mg/mL
C^S_{in}, C^S_{out} = solute concentration in the strip inlet and strip outlet, respectively, mg/mL
C^F_b, C^S_b = solute concentration in the bulk phase for feed and strip, respectively, mg/mL
C^F_i, C^S_i = solute concentration at the fiber inside wall surface in the feed and the strip phases, mg/mL
C^F_m, C^S_m = solute concentration on the feed and the strip side of the bulk membrane phase, mg/mL
C^F_{mi}, C^S_{mi} = solute concentration in the membrane phase at the feed-membrane and at the strip-membrane interfaces, for hydrophobic substrate, mg/mL
C^F_o, C^S_o = solute concentration at the fiber outside wall surface in the feed and the strip phases, mg/mL
d_i, d_o, d_{lm} = hollow fiber inside diameter, outside diameter, and the log-mean diameter, respectively, cm
D_o, D_w = molecular diffusivity of solute in the organic (membrane) phase, and in water, cm^2/s
ΔC_{LM} = log mean concentration difference, Eq. 12c.
k_{mo} = permeability of the organic membrane (D_o/δ_M), cm/s
k^F_w, k^S_w = boundary layer coefficients in the feed and the strip phase, respectively, cm/s
k^F_{sw}, k^S_{sw} = substrate coefficients for hydrophilic water-filled substrate, on the feed and the strip side, respectively, cm/s
k^F_{so}, k^S_{so} = substrate coefficients for hydrophobic organic (membrane)-filled substrate, on the feed and the strip side, respectively, cm/s
K_{s+m} = combined substrate and membrane transfer coefficient, Eqs. 14a and 14b, cm/s
K_w = overall mass transfer coefficient; experimental values defined in Eqs. 12a and 12b, and predicted values defined in Eqs. 6 and 11, for hydrophilic and hydrophobic substrates, respectively, cm/s
L = effective permeation length of the permeator module, cm
m_D = solute distribution coefficient, organic phase concentration to aqueous phase concentration, (mg/L)/(mg/L)
N_F, N_S = total number of feed and strip fibers, respectively, in the module
N_{Re} = Reynolds number, $= 4Q\rho/(60\pi d_i \eta N_T)$; $N_T = N_F$ or N_S
N_{Sc} = Schmidt number, $\eta/\rho D_w$
N_{Sh} = Sherwood number, kd_i/D_w
Q = total mobile phase flow rate (feed or strip), cm^3/min
R_T = solute transfer rate per unit permeator length, Eq. 1, mg/cm · s
t_s = thickness of the substrate, [$=(d_o - d_i)/2$], cm
X = flow variable, Eq. 13

Subscripts and superscripts

expt = experimental values
F, S = feed or strip

Greek letters

δ_M = membrane thickness, cm
ϵ_s = substrate porosity
η = viscosity of the aqueous phase, g/cm · s
θ = variable defined in Eq. 10a

π = 3.1415927 . . .
ρ = density of the aqueous phase, g/cm^3
τ_s = substrate tortuosity factor

Literature Cited

Babcock, W. C., D. J. Brose, A. R. Chambers, and D. T. Friesen, "Separation of Citric Acid From Fermentation Beer Using Supported Liquid Membrane," AIChE Mtg., Boston (Aug., 1986).

Bhave, R. R., and K. K. Sirkar, "Gas Permeation and Separation By Aqueous Membranes Immobilized Across The Whole Thickness Or In A Thin Section of Hydrophobic Microporous Celgard Films," *J. Membrane Sci.*, **27**, 41 (1986).

———, "Gas Permeation and Separation with Aqueous Membranes Immobilized in Microporous Hydrophobic Hollow Fibers," in "Liquid Membranes—Theory and Applications," *ACS Symp. Ser.* **347**, R. D. Noble and J. D. Way, ACS, Washington, DC (1987).

Bloch, R., "Hydrometallurgical Separations By Solvent Membranes," *Membrane Science and Technology*, ed., J. Flynn, Plenum Press, New York (1970).

Cahn, R. P., and N. N. Li, "Separation of Phenol From Waste Water By The Liquid Membrane Technique," *Sep. Sci.*, **9**(6), 505 (1974).

Danesi, P., "Separation of Metal Species By Supported Liquid Membranes," *Sep. Sci. and Tech.*, **19**(11–12), 857 (1984–85).

Danesi, P. R., L. Reichley-Yinger, and P. G. Rickert, "Life-Time of Supported Liquid Membranes: The Influence Of Interfacial Properties, Chemical Composition And Water Transport On The Long-Term Stability of The Membranes," *J. Membrane Sci.*, **31**(2–3), 117 (1987).

Dahuron, L., and E. L. Cussler, "Protein Extraction with Hollow Fibers," *AIChE J.*, **34**, 130 (1988).

Dullien, F. A. L., *Porous Media Fluid Transport and Pore Structure*, 14, Academic Press, New York (1979).

Frank, G. T., and K. K. Sirkar, "Alcohol Production by Yeast Fermentation and Membrane Extraction," *Biotechnol. and Bioeng. Symp. Ser.*, **15**, 621 (1985).

Keller, K. H., and T. R. Stein, "A Two-Dimensional Analysis of Porous Membrane Transport," *Math. Biosci.* **1**, 421 (1967).

Kiani, A., R. R. Bhave, and K. K. Sirkar, "Solvent Extraction with Immobilized Interfaces In a Microporous Hydrophobic Membrane," *J. Membrane Sci.*, **20**(2), 125 (1984).

Kiezyk, P. R., and D. Mackay, "The Screening And Selection of Solvents For The Extraction of Phenol From Water," *Can. J. of Chem. Eng.*, **51**, 741 (1973).

Kuo, Y., and H. P. Gregor, "Acetic Acid Extraction by Solvent Membrane," *Sep. Sci. and Tech.*, **18**(5), 421 (1983).

Lonsdale, H. K., "The Growth of Membrane Technology," *J. Memb. Sci.*, **10**, 81 (1982).

Majumdar, A., and P. Stroeve, "Diffusion of Local Anesthetics Through Liquid Membranes," *J. Memb. Sci.*, **26**, 329 (1986).

Majumdar, S., "A New Liquid Membrane Technique for Gas Separation," *Ph.D. Diss.*, Stevens Inst. of Technol., Hoboken, NJ (1986).

Majumdar, S., A. K. Guha, and K. K. Sirkar, "A New Liquid Membrane Technique For Gas Separation," *AIChE J.*, **34**, 1135 (1988a).

Majumdar, S., A. K. Guha, Y. T. Lee, and K. K. Sirkar. "A Two-Dimensional Analysis of Membrane Thickness in a Hollow Fiber Contained Liquid Membrane Permeator," *J. Memb. Sci.*, submitted, (1988b).

Marr, R., and A. Kopp, "Liquid Membrane Technology—A Survey of Phenomena, Mechanisms, and Models," *Int. Chem. Eng.*, **22**(1), 44 (1982).

Matson, S. L., J. Lopez, and J. A. Quinn, "Separation of Gases with Synthetic Membranes," *Chem. Eng. Sci.*, **38**, 503 (1983).

Nishiki, T., and R. G. Bautista, "Platinum (IV) Extraction with Supported Liquid Membrane Containing Trioctylamine Carrier," *AIChE J.*, **31**, 2093 (1985).

Prasad, R., A. Kiani, R. R. Bhave, and K. K. Sirkar, "Further studies on Solvent Extraction with Immobilized Interfaces in a Microporous Hydrophobic Membrane," *J. Memb. Sci.*, **26**, 79 (1986).

Prasad, R., and K. K. Sirkar, "Microporous Membrane Solvent Extraction," *Sep. Sci. and Tech.*, **22**(2,3), 619 (1987a).

———, "Solvent Extraction with Microporous Hydrophilic and Composite Membranes," *AIChE J.*, **33**, 1057 (1987b).

———, "Dispersion-Free Solvent Extraction with Microporous Hollow Fiber Modules," *AIChE J.*, **34**, 177 (1988).

Reid, R. C., J. M. Prausnitz, and T. K. Sherwood, *The Properties of Gases and Liquids*, 3rd ed., McGraw-Hill, New York (1977).

Skelland, A. H. P., *Diffusional Mass Transfer*, 162, Wiley, New York (1974).

Way, J. D., R. D. Noble, T. M. Flynn, and E. D. Sloan, "Liquid Membrane Transport—A Survey," *J. Memb. Sci.*, **12**, 239 (1982).

Won, K. W., and J. M. Prausnitz, "Distribution of Phenolic Solutes Between Water and Polar Organic Solvents," *J. Chem. Thermody.*, **7**, 661 (1975).

Manuscript received Sept. 23, 1987, and revision received May 16, 1988.